Segmentation of Overlapping Cervical Cells in Microscopic Images with Superpixel Partitioning and Cell-wise Contour Refinement

Hansang Lee Junmo Kim
Korea Advanced Institute of Science and Technology
{hansanglee,junmo.kim}@kaist.ac.kr

Abstract

Segmentation of cervical cells in microscopic images is an important task for computer-aided diagnosis of cervical cancer. However, their segmentation is challenging due to inhomogeneous cell cytoplasm and the overlap between the cells. In this paper, we propose an automatic segmentation method for multiple overlapping cervical cells in microscopic images using superpixel partitioning and cell-wise contour refinement. First, the cell masses are detected by superpixel generation and triangle thresholding. Then, nuclei of cells are extracted by local thresholding and outlier removal. Finally, cell cytoplasm is initially segmented by superpixel partitioning and refined by cell-wise contour refinement with graph cuts. In experiments, our method showed competitive performances in two public challenge data sets compared to the state-of-the-art methods.

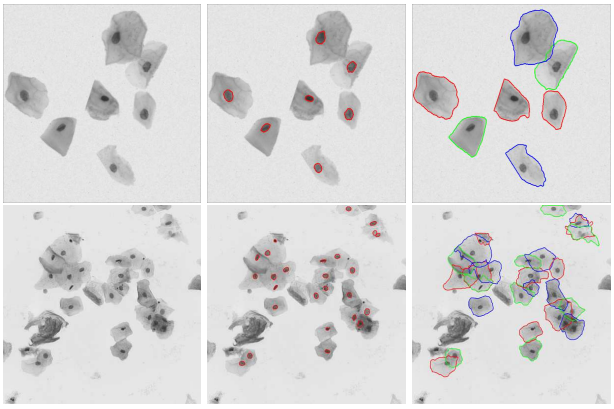

(a) Input images (b) Nuclei (c) Cytoplasm

Figure 1: Examples of microscopic images for overlapping cervical cells, and nucleus and cytoplasm segmentation.

1. Introduction

Analyzing individual cervical cells in microscopic cytology images, obtained from the Pap smear test, is an important task for early diagnosis of cervical cancer [4]. Number and shape of cells are known to be important features for pre-cancerous diagnosis of cervical cancer. However, visual analysis by human experts often suffers from intra- and inter-observer variability. Recently, computer-aided diagnosis and detection have became of interest and numerous attempts have been concentrated on the task of automatic analysis and understanding microscopic images. In cervical cell microscopy, several works such as segmenting cell boundaries, rejecting outliers e.g. blood and mucus, have been studied to support and automate cytology image analysis and cancer diagnosis systems. Detection and segmentation of cervical cells in cytology images, shown in Fig. 1, are however considered to be challenging tasks due to (1) inhomogeneous cell cytoplasm, and (2) the overlap between the cells. First, since the cytoplasm of cell is inhomogeneous, it is not enough to extract the cytoplasm with threshold-based segmentation scheme. Furthermore, since the cells are overlapped in the microscopic image, delineation of cell boundaries in cell overlapping regions is particularly challenging.

Two grand challenges on the segmentation of overlapping cervical cells in microscopic images acquired from Pap smear test, have been recently publicized in ISBI 2014 and ISBI 2015 conferences. On these public data sets, numerous works [13, 8, 5, 9, 11] have addressed the problem in diverse approaches and achieved state-of-the-art-level performances. In Ushizima *et al.* [13], the cell masses were extracted by superpixel clustering and triangle algorithm. Within the extracted cell masses, nuclei were detected by local thresholding, and cytoplasm were partitioned by Voronoi diagram. In Nosrati *et al.* [8], the cell nuclei were detected by combining maximally stable extremal region detector (MSER) [7] and random forest classifier. From these nuclei, cytoplasm was represented as multiple signed distance functions and was segmented by Chan-Vese method [3]. In Lu *et al.* [5], the rough segmentation on cervical cells was first performed including cell mass seg-

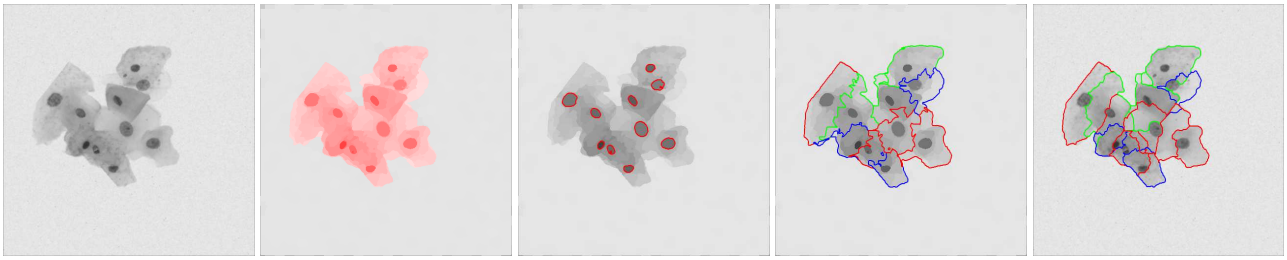

(a) Input image (b) Cell mass detection (c) Nucleus extraction (d) Initial cytoplasm (e) Contour refinement

Figure 2: Overview of our approach; (a) An input image, (b) cell mass detection, (c) nucleus extraction, and cytoplasm segmentation consisting of (d) superpixel partitioning and (e) contour refinement.

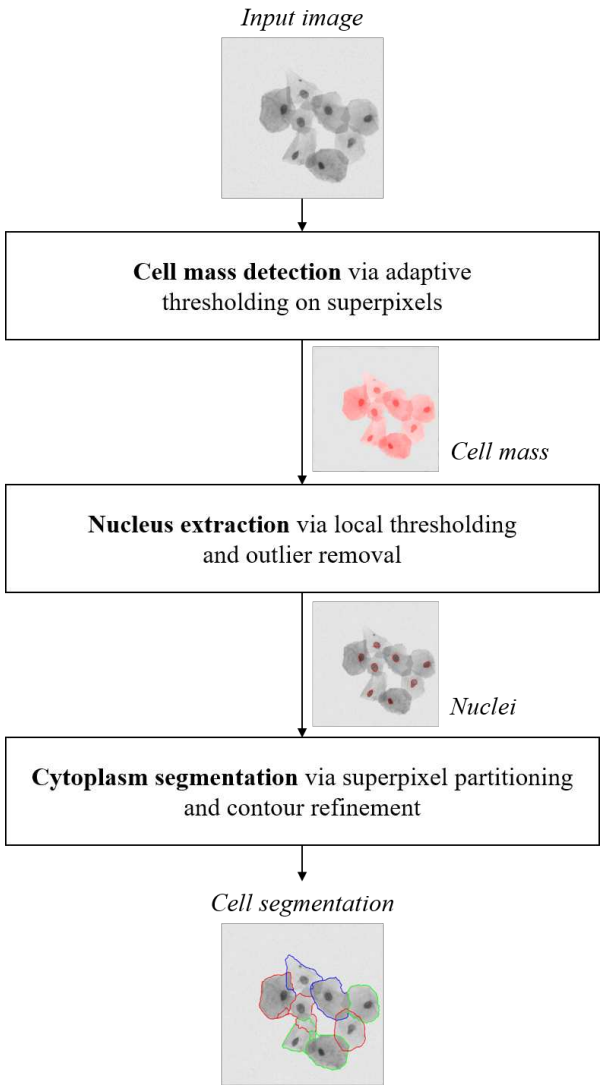

Figure 3: A workflow of the proposed approach.

mentation with quick shift algorithm [14], nuclei detection and segmentation with MSER detector, and initial cell segmentation with shape prior-based level set approach [12]. Cell segmentation was then refined by joint level set representation with geodesic-based shape prior. In Phoulady *et al.* [9], cell nuclei were detected by iterative thresholding and cell masses were segmented by Gaussian mixture model (GMM) estimation. Cytoplasm was then segmented by constructing grid-based distance map on multi-focal images and labeling grids based on these distance maps. In Ramalho *et al.* [11], which is an improved version of Ushizima *et al.* [13], the boundaries of overlapping cells were refined by combining boundary information from extended depth-of-field (EDF) image and multi-focal images. The set of borders detected by Laplacian of Gaussian (LoG) method from multi-focal images and the boundary contours extracted by Canny detector from EDF image were combined to refine the cytoplasm boundaries with morphological reconstruction.

In this paper, we propose an automatic segmentation method of multiple overlapping cervical cells in microscopic images with superpixel partitioning and cell-wise contour refinement. First, to determine the search area, cell masses are detected by superpixel generation and adaptive triangle thresholding. To define the cell placement, nuclei of the cells are extracted by window-based local theshold-ing and outlier removal. Finally, to delineate the boundaries of the overlapping cells, the cell cytoplasm is segmented by superpixel partitioning and cell-wise contour refinement. Experiments demonstrate our method shows competitive results in two public challenge data sets, compared to the state-of-the-art methods. Our major contribution is on superpixel partitioning and contour refinement in cell cytoplasm segmentation, which enhances accuracy of overlapping cell boundaries to the state-of-the-art-level performance, in spite of simple algorithm.

2. Methods

An outline of our approach is summarized in Figures 2 and 3. Our method consists of three major steps: cell mass detection, nuclei extraction, and cytoplasm segmentation.

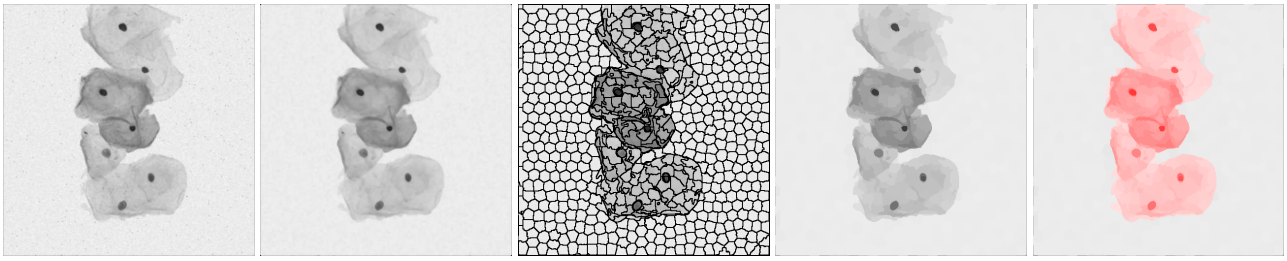

(a) Input image (b) Filtered image (c) Superpixel edges (d) Mean image (e) Cell masses

Figure 4: Cell mass detection; (a) An input image, (b) filtered image, (c) superpixel edge map, (d) mean-value image for superpixels, and (e) detected cell masses.

First, the cell masses including nuclei and cytoplasm are detected by superpixel clustering and adaptive thresholding. From cell masses, the nuclei for cells are extracted by local thresholding and outlier removal. Finally, the cytoplasm of overlapping cells are segmented by superpixel partitioning and contour refinement.

2.1. Cell mass detection

In cell mass detection, entire cell masses including nuclei and cytoplasm of cells are extracted to use the cell mass as region of interest (ROI). First, an input image is noise-reduced by median filter, as shown in Fig. 4 (b), and over-segmented to generate superpixels by SLIC [1] method, as shown in Fig. 4 (c). Then, mean intensity values are computed for each superpixel to generate the mean-value image, as shown in Fig. 4 (d). Cell mass is then extracted by an adaptive thresholding using triangle method [13], as shown in Fig. 4 (e). The extracted cell mass is used as the search area for nucleus extraction and cytoplasm segmentation.

2.2. Nucleus extraction

In nucleus extraction, the nuclei of cells are extracted to locate individual cells in the cell mass. Since the cell nuclei are usually darker than the cytoplasm, as shown in Fig. 1, we extract nuclei by local thresholding [13]. In local thresholding, the threshold T for each superpixel is determined as $T = \mu(1+p\exp(-q\mu)+k(\sigma/s-1))$, where μ, σ are mean and standard deviation of local window intensities, respectively, and $p = 2, q = 10, k = 0.25, s = 1$ are weighting variables. The local window for each superpixel is defined as a group of superpixels whose distances between the centers are less than $d = 0.1 \times l$ where l is image width. With the locally defined threshold T, the superpixels which mean intensities are less than T, are classified as initial nucleus candidates.

Initial nucleus candidates regularly consist of relatively dark spots, however, include also non-nucleus outliers, as shown in Fig. 5 (a). Thus, From the nucleus candidates, outlier removal is performed by (1) breaking superpixel clusters, (2) rejecting tiny superpixels, and (3) rejecting nucleus candidates with low circularity. First, clustered superpixels as shown in Fig. 5 (a), are reduced by rejecting the brightest superpixel iteratively. Since the nucleus often contains at most two superpixels, a superpixel cluster containing more than three superpixels can be considered to have outlier candidates in it. Superpixel clusters are extracted by connected component labeling and for each cluster containing more than three superpixels, a superpixel with the highest mean intensity is rejected. The cluster extraction and superpixel rejection are iteratively repeated until no clusters are extracted.

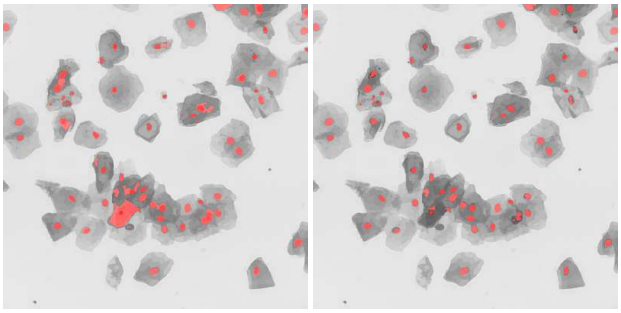

(a) Initial nuclei (b) Final nuclei

Figure 5: Nucleus extraction; (a) Initial nucleus candidates by local thresholding, and (b) finally extracted nuclei by outlier removal.

Second, the superpixel candidates with too small sizes are rejected. In experiments, the superpixels with less than 30 pixels are rejected from the candidates. Finally, the candidates with low circularity are rejected since the nucleus has circular shape. The circularity ρ of a candidate is computed as $\rho = 4\pi A/P^2$ where A, P are the area and the perimeter of a candidate region, respectively. ρ is known to be 1 for perfect circle and much less than 1 for starfish shape. In our approach, the candidate superpixels with $\rho < 0.5$ are rejected. Throughout the outlier removal, finally extracted nuclei consist of most of cell nuclei without

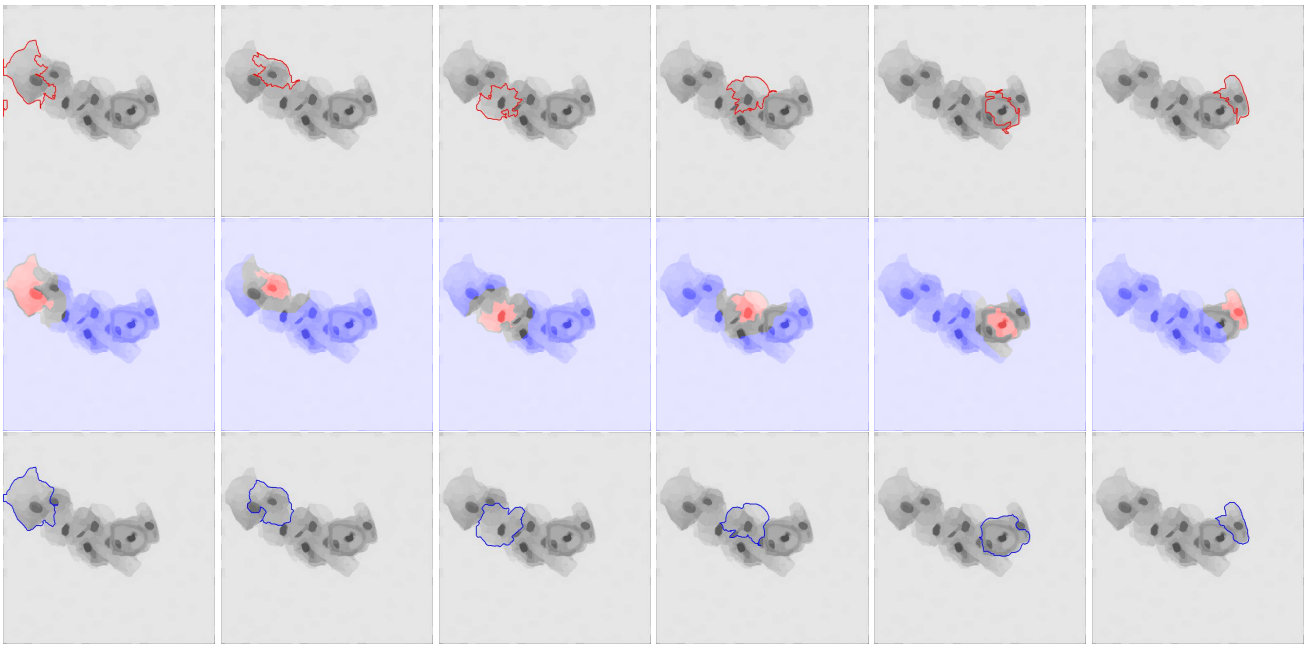

Figure 6: Cell-wise graph cuts for contour refinement in cytoplasm segmentation; Individual cells on the input image by superpixel partitioning (top row), object (red) and background (blue) seed regions generated for cell-wise graph cuts (middle row), and fine-segmented cell contours (bottom row.)

outlier regions as shown in Fig. 5 (b). The extracted nuclei are used as cell indicators in cytoplasm segmentation.

2.3. Cytoplasm segmentation

In cytoplasm segmentation, the boundaries of overlapping cells are determined by superpixel partitioning and cell-wise contour refinement. In superpixel partitioning, the cytoplasm of individual cells are roughly extracted by labeling non-nucleus superpixels into the nearest nucleus, as shown in Fig. 2 (d) and the top row of Fig. 6. These distance-based labels of cytoplasm provide fine initial information of individual cells surrounding nuclei. However they suffer from incorrect and noisy boundaries especially in cell overlapping regions.

Boundaries of cytoplasm in cell overlapping regions are then refined by cell-wise contour refinement. In contour refinement, graph cut segmentation [2] is iteratively performed for each cell individually, to refine the cell contour, as shown in Fig. 6. For each cell, from the initial cell labels extracted by superpixel partitioning, object and background seed for graph cuts are determined by morphological operation, as shown in the middle row in Fig. 6. In graph cuts, only the pair-wise cost term in Boykov *et al.* [2] is used for the cost function to focus on smoothness constraint. Throughout the graph cuts, the contours of individual cells are then refined so that appropriate boundaries of cells are extracted in cell overlapping regions, as shown in the bottom row of Fig. 6.

3. Results

We have tested our approach on data sets used in two recent challenges held in ISBI 2014 [1] and ISBI 2015 [2]. ISBI-14 [6] consists of 945 synthetic and 16 real Pap smear slide images, 135 synthetic and 8 real images used for training and 810 synthetic and other 8 real images used for testing. The synthetic images, as shown in top three rows in Fig. 7, were synthetically generated from real Pap smear slides [6]. In evaluation, 810 synthetic images of 512×512 pixels and their ground truth contours of cell nuclei and cytoplasm were used. ISBI-15 consists of 17 real extended depth of field (EDF) images of 1024×1024 pixels, as shown in bottom three rows in Fig. 7, from which 8 used for training and 9 for testing. For each EDF image in ISBI-15, a set of multi-focal images were additionally provided, but were not used in our experiments. All images were annotated with the ground truths of cell nuclei and cytoplasm.

Our segmentation results were summarized in Fig. 7 and Table 1. In Fig. 7 (b) and (c), cell masses and nuclei were accurately defined by triangle threholding and local thresholding, respectively, in both ISBI-14 and ISBI-15 data sets. In Fig. 7 (d), the initial cytoplasm segmented by superpixel partitioning was well located around the nuclei of individual cells, however cell overlapping regions were omitted and noisy boundaries occurred. In Fig. 7 (e), the boundaries of

[1] http://cs.adelaide.edu.au/ carneiro/isbi14_challenge/index.html
[2] http://cs.adelaide.edu.au/ zhi/isbi15_challenge/index.html

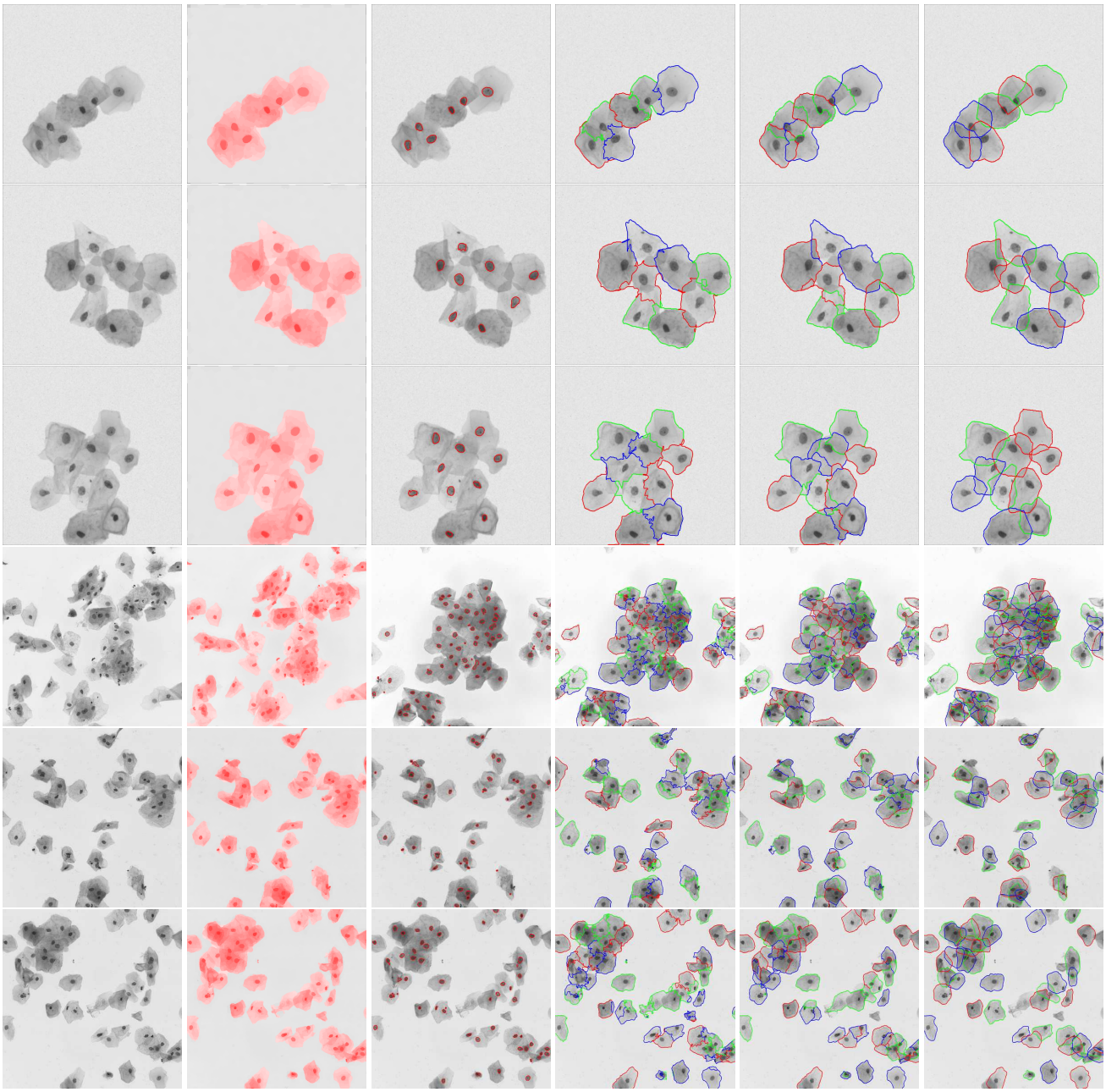

(a) Input images (b) Cell masses (c) Nuclei (d) Spx. partitions (e) Final cytoplasm (f) Ground truths

Figure 7: Examples of our nucleus and cytoplasm segmentation results; (a) Input images, (b) detected cell masses, (c) extracted nuclei, (d) initial cytoplasm candidates by superpixel partitioning, (e) final cytoplasm segmentation, and (f) ground truths.

cell overlapping regions were refined with the help of cell-wise contour refinement, showing successful delineation of overlapping cells. As a result, our method extracted accurate cell cytoplasm similar to the ground truth contours, as shown in Fig. 7 (f).

To validate our method, we evaluated our results by quantitative measurements [6] including the Dice coefficients (DC), object-based false negative (FNo), pixel-based true positive (TPp), and pixel-based false positive rates (FPp) between our cytoplasm segmentation and ground truths, on both ISBI-14 and ISBI-15 data sets. Evaluations were performed on 810 synthetic images in ISBI-14 data set

Table 1: Evaluation and comparison of our cytoplasm segmentation results with the state-of-the-art methods [13, 8, 5, 9, 11] on ISBI-14 and ISBI-15 [6] challenge data sets.

data sets	Methods	DC	FNo	TPp	FPp
ISBI-14	Ushizima *et al.* [13]	0.872 ± 0.082	0.267 ± 0.278	0.841 ± 0.130	0.002 ± 0.003
	Nosrati *et al.* [8]	0.871 ± 0.075	0.111 ± 0.166	0.875 ± 0.086	0.004 ± 0.004
	Lu *et al.* [5]	0.893 ± 0.082	0.316 ± 0.295	0.905 ± 0.096	0.004 ± 0.005
	Spx. partitioning	0.862 ± 0.079	0.235 ± 0.243	0.822 ± 0.122	0.002 ± 0.002
	Our approach	0.897 ± 0.075	0.137 ± 0.194	0.882 ± 0.097	0.002 ± 0.003
ISBI-15	Phoulady *et al.* [9]	0.831 ± 0.079	0.408 ± 0.163	0.927 ± 0.098	0.003 ± 0.002
	Ramalho *et al.* [11]	0.856 ± 0.078	0.501 ± 0.180	0.899 ± 0.113	0.002 ± 0.001
	Spx. partitioning	0.837 ± 0.081	0.546 ± 0.144	0.798 ± 0.134	0.001 ± 0.001
	Our approach	0.879 ± 0.087	0.434 ± 0.168	0.877 ± 0.123	0.001 ± 0.001

and 9 real EDF images in ISBI-15 data set as the challenge policy. In numerical evaluation, the average DC, TPp and FPp were measured over the "good" cell segmentation [10] which is a segmented region with DC>0.7. The object-based FNo was computed as a ratio of cells with DC≤ 0.7.

Table 1 summarizes the numerical evaluation of our segmentation results and comparisons with those of state-of-the-art methods [6, 13, 8, 9, 11]. Due to erroneous boundaries in cell overlapping regions, our initial cytoplasm segmentation by superpixel partitioning, denoted as *Spx. partitioning*, shows relatively low performance with DC of 0.862 ± 0.079, FNo of 0.235 ± 0.243, TPp of 0.822 ± 0.122, and FPp of 0.002 ± 0.002 in ISBI-14, and DC of 0.837 ± 0.081, FNo of 0.546 ± 0.144, TPp of 0.798 ± 0.134, and FPp of 0.001 ± 0.001 in ISBI-15. However, with the help of cell-wise contour refinement, our final segmentation shows fine performance with DC of 0.897 ± 0.075, FNo of 0.137 ± 0.194, TPp of 0.882 ± 0.097, and FPp of 0.002 ± 0.003 in ISBI-14, and DC of 0.879 ± 0.087, FNo of 0.434 ± 0.168, TPp of 0.877 ± 0.123, and FPp of 0.001 ± 0.001 in ISBI-15. In DC, our method achieves the best performance in both ISBI-14 and ISBI-15 data sets by improving the top average scores by 0.4 %p and 2.3 %p in ISBI-14 and ISBI-15, respectively. In other measurements including FNo, TPp, and FPp, our method shows competitive performance compared to the state-of-the-art methods.

4. Discussions

We proposed an automatic segmentation method of overlapping cervical cells in microscopic images. To overcome the challenge of segmenting overlapping multiple cells, we proposed superpixel partitioning and cell-wise contour refinement by graph cuts for cell cytoplasm segmentation. In experiments, our method achieved the best performance in DC metric, and competitive results in other metrics. In ISBI-15 data set, our method showed competitive perfor-

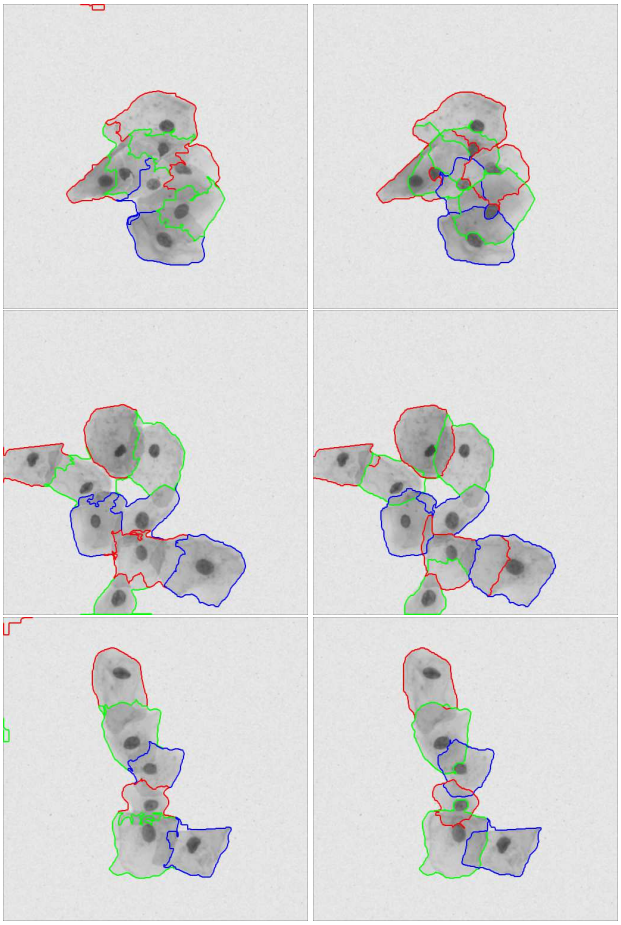

(a) Superpixel partitioning (b) Contour refinement

Figure 8: Effects of superpixel partitioning and cell-wise contour refinement in cytoplasm segmentation; (a) Initial cytoplasm by superpixel partitioning, and (b) final cytoplasm by cell-wise contour refinement.

mance even without using additional multi-focal images, in which comparative methods [9, 11] have used them.

Further visual assessment of our cytoplasm segmentation is summarized in Fig. 8. Based on distance-based partitioned cell cytoplasm, our cell-wise contour refinement with graph cuts enhances cell boundaries especially on the cell-overlapping regions. With the help of graph cuts, outlier cell masses along image boundaries in the first and third rows in Fig. 8 (a), were removed in refinement results. Our contour refinement, however, has a limitation of delineating boundaries along nucleus, as shown in the bottom blue cell in first row and bottom green cell in third row in Fig. 8. The reason for this tendency is that the nucleus has the strongest boundary with large contrast. Shape prior segmentation or nucleus handling can be used to improve the cytoplasm contouring.

In quantitative evaluation, shown in Table 1, the limitations of our method can be discussed. In FNo, our method showed weaker performance than Nosrati *et al.* [8] in ISBI-14 and Phoulady *et al.* [9] in ISBI-15. Furthermore, in TPp, our method performed weaker than Lu *et al.* [5] in ISBI-14, and Phoulady *et al.* [9] and Ramalho *et al.* [11] in ISBI-15. It can be analyzed that (1) our method often extracts false cells due to outlier nuclei detected in nucleus extraction, and (2) non-cytoplasm regions e.g. mucus, blood, and inflammatory cells are included in the cytoplasm of our segmentation results. For further improvement, it is required to enhance the outlier removal in both nucleus detection and cytoplasm segmentation.

5. Conclusion

In summary, we have proposed an automatic segmentation method of overlapping cervical cells in microscopic images. In cell mass detection, we extracted superpixels from a microscopy and performed triangle thresholding to select the cell masses. In nucleus extraction, we have located the cells by indicating cell nuclei with local thresholding and outlier removal. In cytoplasm segmentation, we initially segmented the cytoplasm with superpixel partitioning by labeling superpixels into the cells with nearest nucleus. Finally, the cell-wise contour refinement was performed by cell-wise graph cuts to extract accurate cell boundaries with overlap. In experiments, our method well detected overlapped boundaries of cervical cells in both public challenge data sets, by showing competitive performances and accuracies compared to the state-of-the-art methods. Further improvement by enhancing nuclei extraction and incorporating multi-focal images, and extended analyses on experimental data will be focused as our future works.

References

[1] R. Achanta, A. Shaji, K. Smith, A. Lucchi, P. Fua, and S. Susstrunk. Slic superpixels compared to state-of-the-art superpixel methods. *IEEE Trans. Pattern Anal. Machine Intel.*, 34(11):2274–2282, Nov 2012.

[2] Y. Boykov and M.-P. Jolly. Interactive graph cuts for optimal boundary amp; region segmentation of objects in n-d images. In *Proc. IEEE Intl. Conf. Computer Vision*, volume 1, pages 105–112 vol.1, 2001.

[3] T. F. Chan and L. A. Vese. Active contours without edges. *IEEE Transactions on Image Processing*, 10(2):266–277, Feb 2001.

[4] A. Gentav, S. Aksoy, and S. nder. Unsupervised segmentation and classification of cervical cell images. *Pattern Recognition*, 45(12):4151 – 4168, 2012.

[5] Z. Lu, G. Carneiro, and A. Bradley. An improved joint optimization of multiple level set functions for the segmentation of overlapping cervical cells. *Image Processing, IEEE Transactions on*, 24(4):1261–1272, April 2015.

[6] Z. Lu, G. Carneiro, A. Bradley, D. Ushizima, M. S. Nosrati, A. Bianchi, C. Carneiro, and G. Hamarneh. Evaluation of three algorithms for the segmentation of overlapping cervical cells. *IEEE Journal of Biomedical and Health Informatics*, PP(99):1–1, 2016.

[7] J. Matas, O. Chum, M. Urban, and T. Pajdla. Robust wide-baseline stereo from maximally stable extremal regions. *Image and Vision Computing*, 22(10):761 – 767, 2004.

[8] M. S. Nosrati and G. Hamarneh. A variational approach for overlapping cell segmentation. In *Overlapping Cervical Cytology Image Segmentation Challenge - ISBI 2014*, 2014.

[9] H. A. Phoulady, D. B. Goldgof, L. O. Hall, and P. R. Mouton. An approach for overlapping cell segmentation in multi-layer cervical cell volumes. In *Overlapping Cervical Cytology Image Segmentation Challenge - ISBI 2015*, 2015.

[10] P. Radau, Y. Lu, K. Connelly, G. Paul, A. Dick, and G. Wright. Evaluation framework for algorithms segmenting short axis cardiac mri. *The MIDAS Journal - Cardiac MR Left Ventricle Segmentation Challenge*, 2009.

[11] G. L. B. Ramalho, D. S. Ferreira, A. G. C. Bianchi, C. M. Carneiro, F. N. S. Medeiros, and D. M. Ushizima. Cell reconstruction under voronoi and enclosing ellipses from 3d microscopy. In *Overlapping Cervical Cytology Image Segmentation Challenge - ISBI 2015*, 2015.

[12] M. Rousson and N. Paragios. *Computer Vision — ECCV 2002: 7th European Conference on Computer Vision Copenhagen, Denmark, May 28–31, 2002 Proceedings, Part II*, chapter Shape Priors for Level Set Representations, pages 78–92. Springer Berlin Heidelberg, Berlin, Heidelberg, 2002.

[13] D. M. Ushizima, A. G. C. Bianchi, and C. M. Carneiro. Segmentation of subcellular compartments combining superpixel representation with voronoi diagrams. In *Overlapping Cervical Cytology Image Segmentation Challenge - ISBI 2014*, 2014.

[14] A. Vedaldi and S. Soatto. *Computer Vision – ECCV 2008: 10th European Conference on Computer Vision, Marseille, France, October 12-18, 2008, Proceedings, Part IV*, chapter Quick Shift and Kernel Methods for Mode Seeking, pages 705–718. Springer Berlin Heidelberg, Berlin, Heidelberg, 2008.